Available online at http://www.journalcra.com

International Journal of Current Research
Vol. 5, Issue, 03, pp.508-513, March, 2013

INTERNATIONAL JOURNAL OF CURRENT RESEARCH

ISSN: 0975-833X

RESEARCH ARTICLE

LAMINAR FREE AND FORCED CONVECTIVE FLOW BETWEEN TWO VERTICAL PLATES EMBEDDED IN POROUS MEDIUM

***,[1]Sanatan Das, [2]Mrinal Jana and [3]Rabindra Nath Jana**

[1]Department of Mathematics, University of Gour Banga, Malda 732 103, West Bengal, India
[2,3]Department of Applied Mathematics, Vidyasagar University, Midnapore 721102, West Bengal, India

ARTICLE INFO

Article History:
Received 25th December, 2012
Received in revised form
24th January, 2013
Accepted 18th February, 2013
Published online 19th March, 2013

Key words:
Free and forced convection,
Grashof number,
critical Grashof number,
porosity parameter and porous medium.

ABSTRACT

Laminar free and forced convective fully developed flow of a viscous incompressible fluid between two infinitely long vertical plates heated asymmetrically embedded in porous medium has been studied. It is observed that the fluid velocity decreases near the channel walls whereas a it increases at the middle region of the channel with an increase in porosity of the medium. The expressions for wall shear stresses, critical Grashof number and the bulk temperature are also derived. It is observed that the bulk temperature increases with increase in either Grashof number or porosity parameter. Further, the critical Grashof number for which there is no flow reversal near the cold wall increases with an increase in temperature ratio parameter while it decreases with an increase in porosity of the medium.

INTRODUCTION

Flow through porous media has been a topic of longstanding interest in many areas of science and engineering. Due to its broad range of applications in science and industry, this field has gained extensive attention lately. In a broader sense, the study of porous media embraces fluid and thermal sciences, geothermal, petroleum and combustion engineering. The flows through porous media have importance to the petroleum engineering concerned with the movement of oil and gas through the reservoir. The topic of porous medium has been well surveyed by (Nield and Bejan 1992; Bejan 1994; Kaviany 1995; Ingham and Pop 2002; Kaviany 1985) has presented an analytical solution for laminar flow through a porous channel bounded by isothermal parallel plates based on the Brinkman-extended Darcy law. Vafai and Kim (1989) have reported a closed-form solution for forced convection flow in a porous channel with isoflux boundaries using the Brinkman-Forchheimer-extended Darcy law. (Poulikakos and Renken 1987; Renken and Poulikakos 1988) have studied, respectively, numerically and experimentally forced convection in a channel filled with a porous medium using the Brinkman-Forchheimer-extended Darcy model with variable porosity and allowing for viscosity variations. Kou and Lu (1993) have analyzed combined boundary and inertia effects for fully-developed mixed convection in a vertical channel embedded in porous media. Cheng *et al*. (1990) have discussed flow reversal and heat transfer of fully-developed mixed convection in vertical channel. Chamkha (1997) has analyzed the problem of hydromagnetic non-Darcy mixed convection flow through a porous medium channel in the presence of heat generation effects. Klemp *et al.* (1990) have investigated the effects of temperature-dependent viscosity on the flow in the entrance region of a channel. The laminar convection through porous medium between two vertical parallel plates with heat source has been studied by (Vidhya and Kesavan 2010). Umavathi (2011) has discussed the free convection of composite porous medium in a vertical channel. Moh'd Ahmad Al-Nimr and Tariq Darabseh (2011) have obtained the analytical solution to transient laminar fully developed free convection in open-ended vertical channel embedded in porous media. Aung (1972) has studied the fully developed laminar free convection between infinitely long vertical plates with asymmetric heating of the plates.

The aim of the present paper is to study free and forced convection of a viscous incompressible fluid flow between two infinitely long vertical plates embedded in a porous medium. It is found that for small values of Grashof number Gr, the velocity distribution decreases near the channel walls while it increases at the middle of the channel with increase in porosity parameter σ. For large values of Grashof number Gr, the effect of porosity of the medium is prominent near the cold wall while near the hot wall the velocity distribution is nearly unaffected by the porosity of the medium. The critical value of the buoyancy force for which there is no flow reversal near the cold wall increases with increase in temperature ratio parameter while it decreases with increase in porosity of the medium. Further, the bulk temperature θ_b increases with an increase in either Grashof number Gr or porosity parameter σ.

Mathematical Formulation and its solution

Consider the fully developed flow of a viscous incompressible fluid between two infinitely long vertical plates embedded in porous medium. The distance between the plates is d. The origin being taken at the left plate of the channel, x-axis is along the walls in the direction of the flow and y-axis perpendicular to it. For fully developed steady flow all physical quantities will be function of y only. The plate at $y = 0$ has a uniform temperature T_2 while the

Corresponding author: jana261171@yahoo.co.in

plate at $y = d$ is subjected to a uniform temperature T_1 where $T_1 > T_2$. It is assumed that the forced convection flow entering the channel is directed vertically upwards whereas the pure free convection is motivated by a zero pressure gradient.

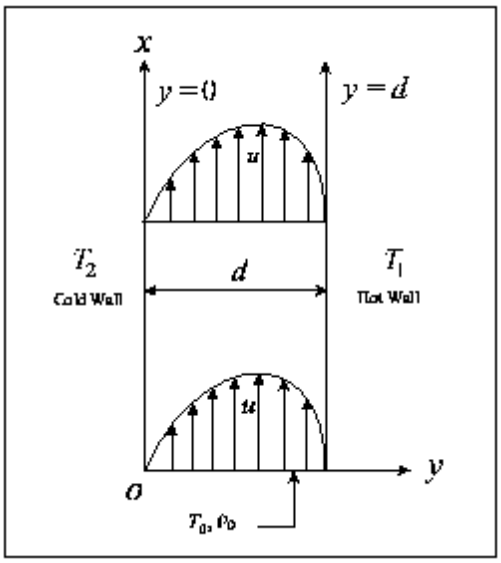

Fig. 1. Geometry of the problem

The equation of motion is

$$0 = -\frac{\partial p^*}{\partial x} + \bar{\mu}\frac{d^2u^*}{dy^2} - \frac{\mu}{k}u^* + \rho_0 g\beta(T - T_0), \tag{1}$$

where $p^* = p + \rho_0 g x$, $\bar{\mu}$ the viscosity of the fluid, μ the viscosity of the porous medium, k the porosity of the medium, g acceleration due to gravity, β the thermal expansion co-efficient, rho_fluid density and T_0 the temperature at the channel entrance.

On neglecting, viscous dissipation, the energy equation is

$$0 = \frac{d^2T}{dy^2}. \tag{2}$$

The velocity and the temperature boundary conditions are

$$u^* = 0 \quad \text{at} \quad y = 0 \text{ and } u^* = 0 \text{ at } y = d,$$

$$u^* = 0 \quad \text{at} \quad y = 0 \text{ and } u^* = 0 \quad \text{at} \quad y = d, \tag{3}$$

$$T = T_2 \text{ at } y = 0 \text{ and } T = T_1 \quad \text{at} \quad y = d. \tag{4}$$

Introducing non-dimensional variables

$$\eta = \frac{y}{d},\ u = \frac{u^* d}{\nu},\ Gr = \frac{g\beta d^3(T_1 - T_0)}{\nu^2},$$
$$\nu = \frac{\bar{\mu}}{\rho_0},\ \theta = \frac{T - T_0}{T_1 - T_0},\ \sigma^2 = \frac{\mu d^2}{\bar{\mu}k},\ r_T = \frac{T_2 - T_0}{T_1 - T_0}, \tag{5}$$

equations (1) and (2) become

$$\frac{d^2u}{d\eta^2} - \sigma^2 u = -(Gr\theta + \alpha), \tag{6}$$

$$\frac{d^2\theta}{d\eta^2} = 0, \tag{7}$$

where $\alpha = -\frac{d^3}{\bar{\mu}\nu}\frac{dp^*}{dx}$ is the non-dimensional pressure gradient.

On the use of (5), the boundary conditions (3) and (4) become

$$u(0) = 0 = u(1), \tag{8}$$

$$\theta(0) = r_T,\ \theta(1) = 1. \tag{9}$$

The solution of the equation (7) subject to the boundary condition (9) is

$$\theta(\eta) = (1 - r_T)\eta + r_T. \tag{10}$$

Equation (10) shows that the temperature distribution is linear. Substituting the value of $\theta(\eta)$ in the equation (6), one can obtain

$$\frac{d^2u}{d\eta^2} - \sigma^2 u = -Gr(1 - r_T)\eta - (Gr r_T + \alpha). \tag{11}$$

Equation (11) together with the boundary condition (8) can be solved easily and the solution for velocity distribution is

$$u(\eta) = \frac{1}{\sigma^2}\Big[(Gr r_T + \alpha) \times \Big\{(1 - \cosh\sigma\eta) - (1 - \cosh\sigma)\frac{\sinh\sigma\eta}{\sinh\sigma}\Big\} + Gr(1 - r_T)\{\eta - \frac{\sinh\sigma\eta}{\sinh\sigma}\Big\}\Big] \tag{12}$$

The velocity distribution depends on the porosity parameter σ. It is noticed that the buoyancy force is balanced by the constant rate of flow. It is seen from the solution (12) that the parameter α is still unknown.

On the use of the mass flow rate

$$\int_0^1 u\, d\eta = 1, \tag{13}$$

the unknown pressure parameter α can be expressed in the following form

$$\alpha = \frac{\sigma^3 \sinh\sigma}{\sigma\sinh\sigma + 2(1 - \cosh\sigma)} - \frac{1}{2}Gr(1 + r_T). \tag{14}$$

On the use of (14), equation (12) becomes

$$u(\eta) = \frac{1}{\sigma^2}\Bigg[\Bigg\{\frac{\sigma^3\sinh\sigma}{\sigma\sinh\sigma + 2(1 - \cosh\sigma)} - \frac{1}{2}Gr(1 - r_T)\Bigg\} \times \Big\{(1 - \cosh\sigma\eta) - (1 - \cosh\sigma)\frac{\sinh\sigma\eta}{\sinh\sigma}\Big\} + Gr(1 - r_T)\Big(\eta - \frac{\sinh\sigma\eta}{\sinh\sigma}\Big)\Bigg]. \tag{15}$$

It is interesting to note from equation (15) that the velocity distribution for $Gr = 0$ (pure forced convection) for any values of

r_T and for $r_T = 1$ with any values of Gr are identical and it becomes

$$u(\eta) = \frac{\sigma[(1-\cosh\sigma\eta)\sinh\sigma - (1-\cosh\sigma)\sinh\sigma\eta]}{\sigma\sinh\sigma + 2(1-\cosh\sigma)}. \quad (16)$$

In the free convection process, letting $\alpha = 0$ in the equation (12), we have the axial velocity distribution as

$$u(\eta) = \frac{Gr}{\sigma^2}\left[r_T\left\{(1-\cosh\sigma\eta) - (1-\cosh\sigma)\frac{\sinh\sigma\eta}{\sinh\sigma}\right\} + (1-r_T)\left\{\eta - \frac{\sinh\sigma\eta}{\sinh\sigma}\right\}\right]. \quad (17)$$

For free convection flow when $r_T = 1$, the solution (17) reduced to

$$u(\eta) = \frac{Gr}{\sigma^2\sinh\sigma}\left[(1-\cosh\sigma\eta)\sinh\sigma - (1-\cosh\sigma)\sinh\sigma\eta\right]. \quad (18)$$

For free and forced convection flow when $\sigma = 1$, the velocity distribution and the pressure gradient are given by

$$u(\eta) = \eta\left[6(1-\eta) - \frac{\sigma^2}{10}(5\eta^3 - 10\eta^2 + 6\eta - 1)\right] - \frac{1}{2}Gr(1-r_T)\eta\left[\frac{1}{6}(2\eta^2 - 3\eta + 1) + \frac{\sigma^2}{360}(6\eta^4 - 15\eta^3 + 10\eta^2 - 1)\right] \quad (19)$$

and

$$\alpha = 12\left(1 + \frac{\sigma^2}{10}\right) - \frac{1}{2}Gr(1+r_T). \quad (20)$$

Letting limit $\sigma \to 0$ in equations (19) and (20), we have

$$u(\eta) = 6\,\eta(1-\eta) - \frac{1}{12}Gr(1-r_T)\eta(2\eta^2 - 3\eta + 1), \quad (21)$$

$$\alpha = 12 - \frac{1}{2}Gr\,(1+r_T). \quad (22)$$

It is seen from (19) that either $Gr = 0$ $Gr<<0$ (pure forced convection) or $r_T = 1$, we have the same velocity distribution

$$u(\eta) = \eta\left[6\eta(1-\eta) - \frac{\sigma^2}{10}(5\eta^3 - 10\eta^2 + 6\eta - 1)\right]. \quad (23)$$

Further, for free convection ($\alpha = 0$), we have, for σ << 0,

$$u = Gr\left[\left\{\frac{1}{2}r_T(\eta - \eta^2) + \frac{1}{6}(1-r_T)(\eta - \eta^3)\right\} - \sigma^2\left\{\frac{r_T}{24}(\eta^4 - 2\eta^3 + \eta) + \frac{(1-r_T)}{360}(3\eta^5 - 10\eta^3 + 7\eta)\right\}\right]. \quad (24)$$

In the limit $\sigma \to 0$, for viscous fluid

$$u(\eta) = \frac{1}{2}Gr[r_T(\eta - \eta^2) + \frac{1}{3}(1-r_T)(\eta - \eta^3)]. \quad (25)$$

Equation (25) is identical with equation (17a) of Aung (1972).

RESULTS AND DISCUSSION

We have presented the non-dimensional velocity $u(\eta)$ for several values of Gr, r_T and σ against η in Figures 2-7. It is observed from Figures 2-7 that the velocity distributions become asymmetric in the presence of buoyancy forces $(Gr \neq 0)$ whether the values of Grashof number Gr are small or large. It is seen from Figures 2 and 3 that the fluid velocity $u(\eta)$ decreases in the left half of the channel and increases in the right half of the channel with increase in Grashof number Gr, for both small as well as large values of Grashof number Gr. It is also seen that for large values of Grashof number Gr, the asymmetric nature of the velocity distributions is more prominent than small values of Gr. An increase in Grashof number Gr leads to an increase in velocity, this is because, increase in Gr means more heating and less density.

Figures 4 and 5 show that with an increase in temperature ratio parameter r_T, the fluid velocity $u(\eta)$ increases in the left half of the channel while it decreases in the right half of the channel for both small and large values of Grashof number Gr. The velocity distribution is asymmetric prominently for large values of Grashof number Gr shown in Figure 5. It is interesting to see from Figure 6 that for small values of Grashof number Gr, the fluid velocity decreases near the channel walls while it increases at the middle of the channel with increase in porosity parameter σ. Further, for small values of Gr, the velocity distribution is symmetrical at the channel in the presence of porous medium. On the other hand, Figure 7 reveals that the fluid velocity distribution is asymmetric in nature for large values of Grashof number Gr. It is also shown that the effect of porosity parameter σ is prominent near the left wall of the channel while near the right wall, the fluid velocity is nearly unaffected by the porosity of the medium. Porous medium produces a resisting force in the flow field. So, as the porosity parameter increases, the resistance in the flow field decreases and as such velocity increases.

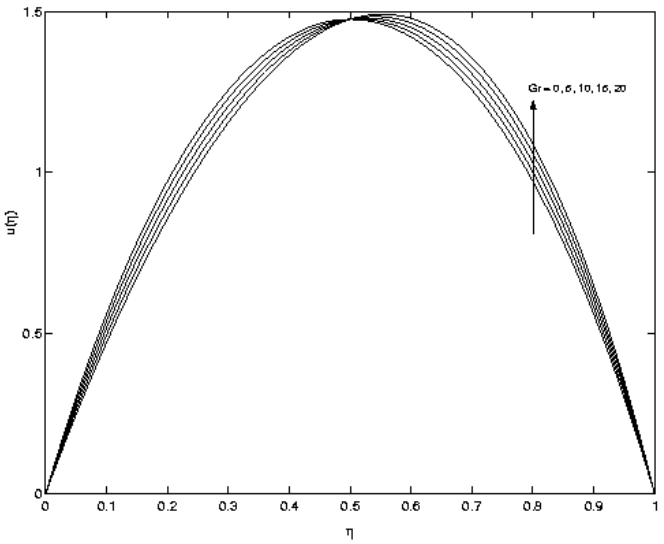

Fig. 2. Velocity profiles for small Gr with $\sigma = 0.5$ and $r_T = 0.2$

The shear stresses at the plates $\eta = 0$ and $\eta = 1$ are given by

$$\left.\frac{du}{d\eta}\right]_{\eta=0} = \frac{1}{2\sigma^2\sinh\sigma}\left[Gr(1-r_T)(2\sinh\sigma - \sigma\cosh\sigma - \sigma) - 2\lambda\sigma(1-\cosh\sigma)\right], \quad (26)$$

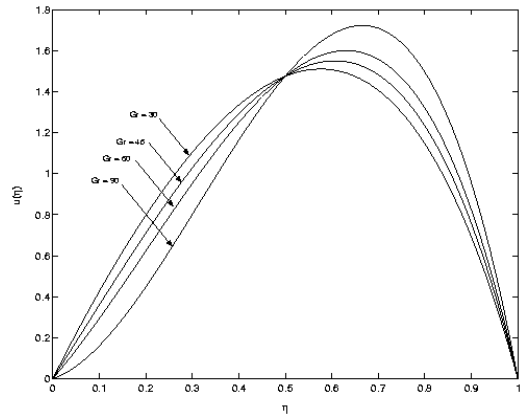

Fig. 2. Velocity profiles for small Gr with $\sigma = 0.5$ and $r_T = 0.2$

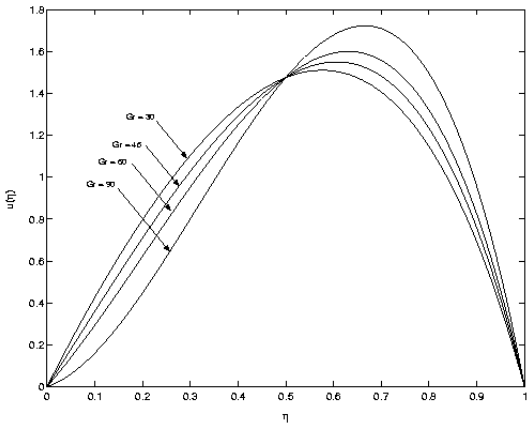

Fig. 3. Velocity profiles for large Gr with $\sigma = 0.5$ and $r_T = 0.2$

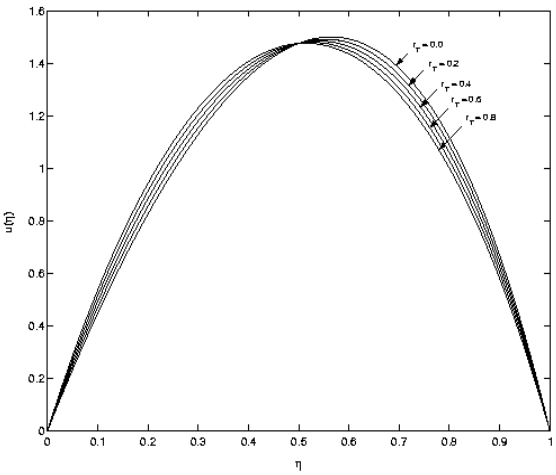

Fig. 4. Velocity profiles for r_T with $\sigma = 0.5$ and small $Gr = 20$

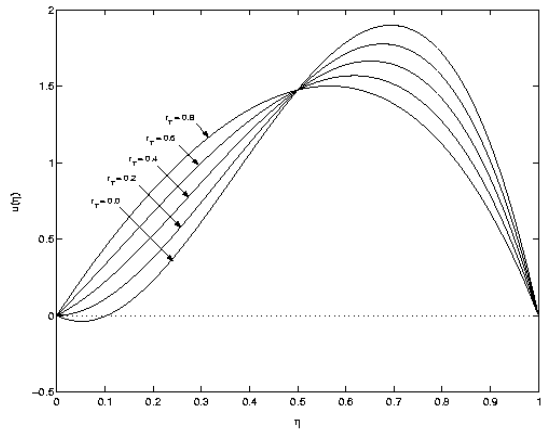

Fig. 5. Velocity profiles for r_T with $\sigma = 0.5$ and large $Gr = 102$

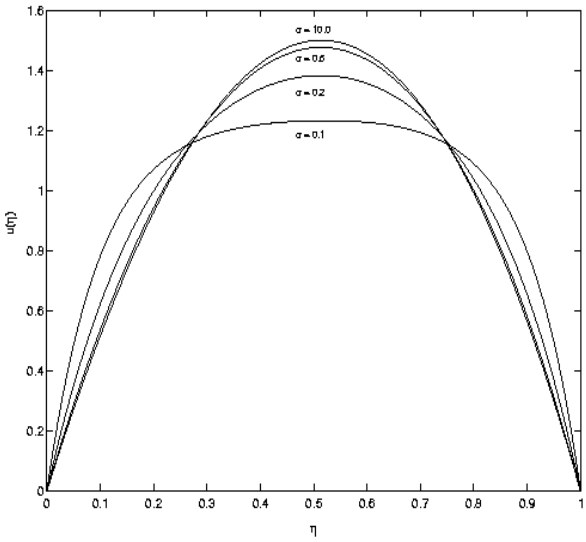

Fig. 6. Velocity profiles for σ with small $Gr = 5$ and $r_T = 0.2$

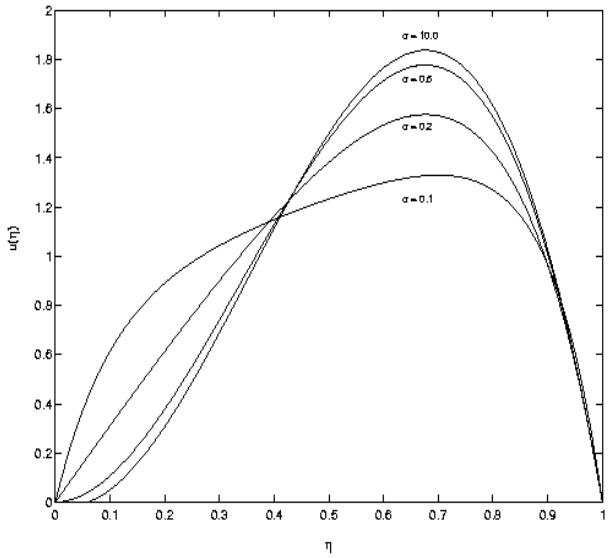

Fig. 7. Velocity profiles for σ with large $Gr = 102$ and $r_T = 0.2$

$$\frac{du}{d\eta}\Big]_{\eta=1} = \frac{1}{2\sigma^2 \sinh\sigma}[Gr(1-r_T)(2\sinh\sigma - \sigma\cosh\sigma - \sigma) + 2\lambda\sigma(1-\cosh\sigma)], \quad (27)$$

where

$$\lambda = \frac{\sigma^3 \sinh\sigma}{\sigma\sinh\sigma + 2(1-\cosh\sigma)}. \quad (28)$$

The numerical values of the shear stresses τ_0 and τ_1 at the plates $\eta = 0$ and $\eta = 1$ respectively are shown in the Figures 8-11 against r_T for several values of σ and Gr. Figures 8 and 9 show that the shear stress τ_0 at the plate $\eta = 0$ decreases with increase in either Gr or σ. Further, for fixed values of Gr and σ, τ_0 steadily increases with increase in temperature ratio parameter r_T. Figures 10 and 11 show that the effects of Gr, σ and r_T on the shear stress at the plate $\eta = 1$ is reversed as that of the plate $\eta = 0$.

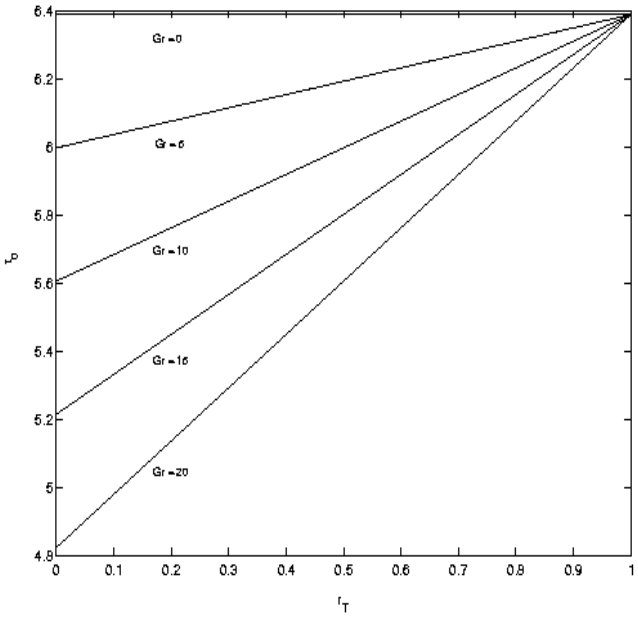

Fig. 8. Shear stress τ_0 for Gr with $\sigma = 0.5$

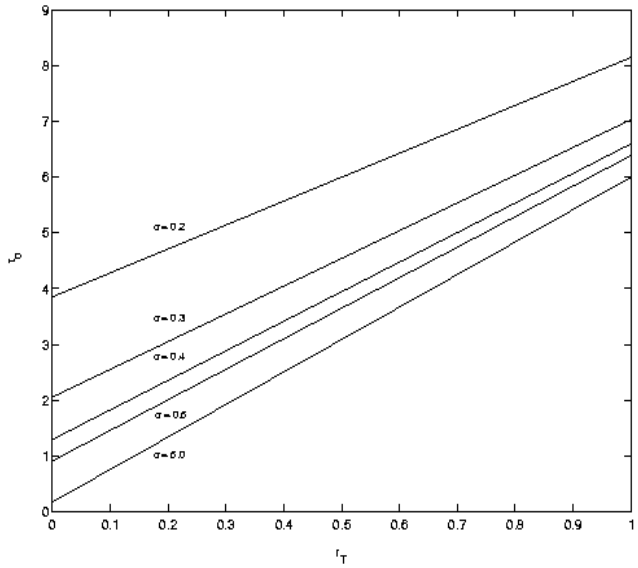

Fig. 9. Shear stress τ_0 for σ with $Gr = 70$

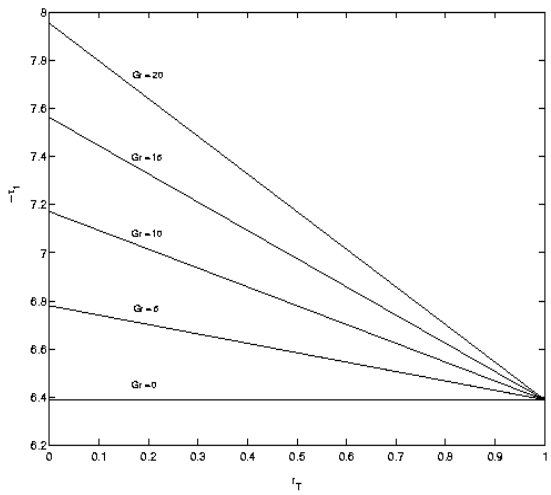

Fig. 10. Shear stress $-\tau_1$ for Gr with $\sigma = 0.5$.

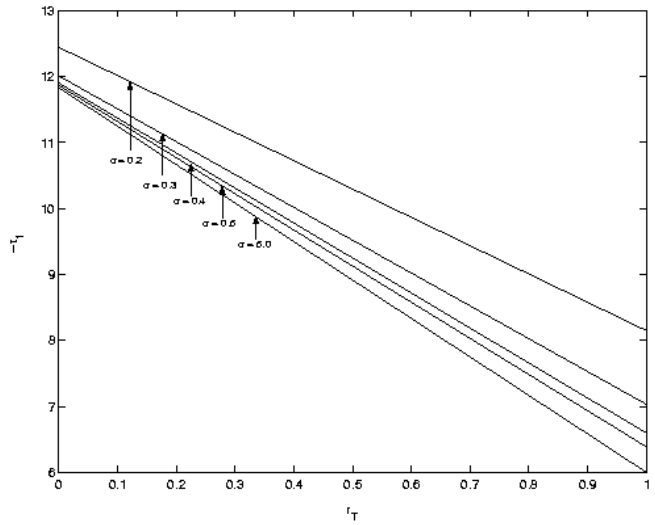

Fig. 11. Shear stress $-\tau_1$ for σ with $Gr = 70$

The critical value of Gr_0 for which there is no flow reversal near the plate $\eta = 0$ is obtained from

$$\frac{du}{d\eta}]_{\eta=0} = 0, \tag{29}$$

which in turn yields

$$Gr_0 = \frac{2\lambda\sigma(1-\cosh\sigma)}{(1-r_T)[2\sinh\sigma - \sigma(1+\cosh\sigma)]}, \tag{30}$$

where λ is given by (28). The corresponding value of the critical Grashof number at the plate $\eta = 1$ is given by $Gr_1 = -Gr_0$. The values of the critical Grashof number Gr_0 are entered in Table 1 for different values of σ and r_T. It is seen from Table 1 that the critical Grashof number Gr_0 at the plate $\eta = 0$ increases with increase in temperature ratio parameter r_T while it decreases with increase in porosity parameter σ.

Table 1. The critical Grashof number $10^{-3} \times Gr_0$

$r_T \setminus \sigma$	0.1	0.5	2.0	10.0
0.0	0.31242	0.08164	0.07260	0.07201
0.2	0.39054	0.10205	0.09075	0.09002
0.4	0.52071	0.13607	0.12100	0.12002
0.6	0.78107	0.20410	0.18150	0.18004

The non-dimensional bulk temperature of the viscous flow through porous medium may be expressed in the following way

$$\theta_b = \int_0^1 u\,\theta\, d\eta \Big/ \int_0^1 u d\eta, \tag{31}$$

which in turn gives

$$\theta_b = \frac{1}{\left[2\alpha + Gr(1+r_T)\right]}\Big[\left\{\alpha(1+r_T) + 2Gr\, r_T\right\} + Gr(1-r_T)^2 \times \frac{2(\sigma^2\sinh\sigma - 3\sigma\cosh\sigma + 3\sinh\sigma)}{3\sigma(\sigma\sinh\sigma - 2\cosh\sigma + 2)}\Big]. \tag{32}$$

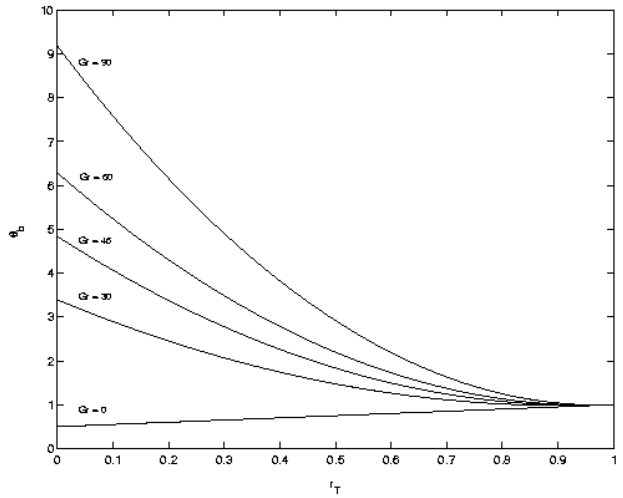

Fig. 12. Bulk temperature distribution θ_b for Gr with $\sigma = 0.5$

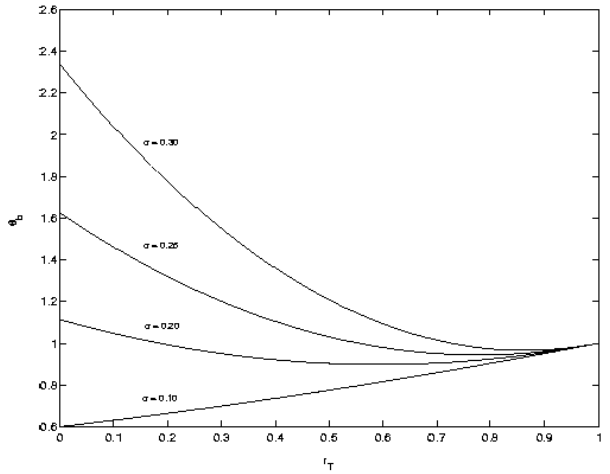

Fig. 13. Bulk temperature distribution θ_b for σ with $Gr = 70$

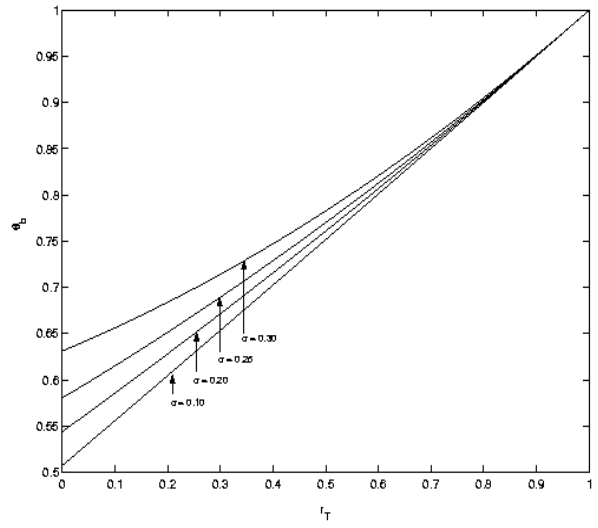

Fig. 14. Bulk temperature distribution θ_b for σ with $Gr = 5$

The numerical values of the bulk temperature θ_b are presented in Figures 12 -14 for several values of σ and Gr against r_T. Figures 12 and 13 show that the bulk temperature the bulk temperature θ_b increases with an increase in either Grashof number Gr or porosity parameter σ. It is also seen that for fixed values of Gr and σ, the bulk temperature θ_b decreases with an increase in temperature ratio parameter and finally converges when $r_T = 1$. Further, the variation of the bulk temperature is linear either for $Gr = 0$ or for small values of the porosity parameter σ. For small values of Gr, it is observed from Figure 14 that the bulk temperature θ_b increases with an increase in temperature ratio parameter r_T.

Conclusion

The steady laminar free and forced convective flow of viscous incompressible fluid between two infinitely long vertical plates embedded in porous medium has been investigated. It is found that the velocity distribution shows asymmetric nature for large values of buoyancy force Gr. In the presence of porous medium, the velocity distribution is symmetric for small values of Grashof number Gr while it is asymmetric for large values of Gr. The critical Grash of number for which there is no flow reversal near the cold wall $(\eta = 0)$ decreases with increase in porosity of the medium. The bulk temperature θ_b increases with an increase in either Grashof number Gr or porosity parameter σ.

REFERENCES

Aung, W., 1972, Fully developed laminar free convection between vertical plates heated asymmetrically, *Heat Mass Tran.*, 15, pp.1577-1580.

Bejan, A., 1994 "Convection heat transfer," Weiley, New York.

Chamkha, A.J., 1997 Non-Darcy fully developed mixed convection in a porous medium channel with heat generation/absorption and hydromagnetic effects. *Numerical Heat Transfer*, Vol. 32, pp.653-675.

Cheng, C.H., Kou, H.S., Huang, W.H., 1990 Flow reversal and heat transfer of fully developed mixed convection in vertical channels. *AIAA J Thermophysics*, Vol. 4 No.3, pp.375-383.

Ingham, D. B. and Pop, I., 2002 Transport phenomena in porous media-II, Elsevier science Ltd., The Boulevard, Langford Lane, Kindlington, Oxford OX5, 1GB, UK.

Kaviany, M., 1995 "Principles of heat transfer in porous media, " Springer-Verley, New York, Inc..

Kaviany, M., 1985 Laminar flow through a porous channel bounded by Isothermal parallel plates. *Int. J. Heat Mass Transfer*, Vol. 28, pp.851-858.

Klemp, K., Herwig, H., Selmann, M., 1990 Entrance flow in a channel with temperature dependent viscosity including viscous dissipation effects, Proceedings of the Third Inte. Cong. Fluid *Mech., Cairo*, Vol. 3, pp.1257-1266.

Kou, H.S., Lu, K.J., 1993 Combined boundary and inertia effects for fully developed mixed convection in a vertical channel embedded in porous media, Int. Commun. Heat Mass Transfer, Vol. 20, pp.333-345.

Moh'd Ahmad Al-Nimr, Tariq Darabseh, 2011. Analytical solution to transient laminar fully developed free convection in open-ended vertical channel embedded in porous media. *Int. J. Appl. Mech. Engng.*, Vol. 2, No. 1, pp. 9-32.

Nield, D. A. and Bejan, A., 1992 "Convection in Porous media," Springer, Berlin, Heidelberg, New York.

Poulikakos, D., Renken, K., 1987 Forced conecvtion in a channel filled with porous medium, including the effects of flow inertia, variable porosity, and Brinkman friction. *Trans. ASME, J. Heat Transfer*, Vol. 109, pp.880-888.

Renken, K., Poulikakos, D., 1988. Experiment and analysis of forced convective heat transport in a packed bed of spheres. *Int. J. Heat Mass Transfer*, Vol.31, pp.1399-1408.

Umavathi, J. C., 2011 Free convection of composite porous medium in a vertical channel. *Heat Transfer-Asian Research*, Vol. 40, No. 4, pp.308-329.

Vafai, K., Kim, S.J. 1989. Forced convection in a channel filled with a porous medium: an exact solution. *Trans. ASME, J. Heat Transfer*, Vol. 111, pp.1103-1106.

Vidhya, M. and Kesavan, S. 2010 Laminar convection through porous medium between two vertical parallel plates with heat source. *Front. Automo. Mech. Engng.*, Vol. 25-27, pp.197-200.

****